

Improved analysis of SN1987A antineutrino events

G. Pagliaroli,^{1,2,*} F. Vissani,^{1,†} M. L. Costantini,^{1,2,‡} and A. Ianni^{1,§}

¹*INFN, Laboratori Nazionali del Gran Sasso, Assergi (AQ), Italy*

²*University of L'Aquila, Coppito (AQ), Italy*

(Dated: August 15, 2018)

We propose a new parameterization of the antineutrino flux from core collapse supernovae, that allows an interpretation of its astrophysical parameters within the Bethe and Wilson scenario for the explosion, and that leads to a reasonable (smooth) behavior of the average energy and of the luminosity curve. We apply it to analyze the events observed by Kamiokande-II, IMB and Baksan detectors in correlation with SN1987A. For the first time, we consider in the same analysis all data characteristics: times, energies and angles of the observed events. We account for the presence of background and evaluate the impact of neutrino oscillations. The hypothesis that the initial luminous phase of emission (accretion) is absent can be rejected at the 2% significance level. Without the need to impose external priors in the likelihood analysis, the best-fit values of the astrophysical parameters are found to be in remarkable agreement with the expectations of the standard core-collapse scenario; in particular, the electron antineutrino-sphere radius is 16 km, the duration of the accretion phase is found to be 0.55 s, and the initial accreting mass is $0.22 M_{\odot}$. Similarly the total energy emitted in neutrinos is 2.2×10^{53} erg, again close to the expectations. The errors on the parameters are evaluated and found to be relatively large, consistently with the limited number of detected events; the two dimensional confidence regions, that demonstrate the main correlations between the parameters, are also given.

PACS numbers: 97.60.Bw Supernovae; 26.30.Jk Weak interaction and neutrino induced processes; 95.55.Vj Neutrino detectors; 14.60.Pq Neutrino mass and mixing.

I. INTRODUCTION

We begin recalling the interest of core collapse supernovae, the status of their understanding, and the expectations for neutrino emission in the standard scenario. Next, we discuss in Sect. IB the motivations for an improved analysis of SN1987A observations in the context of the standard scenario. Finally, we offer an outline of the present investigation.

A. Neutrino emission in core collapse supernovae

Core collapse supernovae (SN) are astrophysical events in which all known forces interplay with each other in extreme physical conditions. An adequate modeling of the processes occurring during this event would be important to obtain information on the left-over compact star [1], on nucleosynthesis [2, 3, 4], on the properties of the supernova remnant [5], and on the expected signals during the explosion; in particular, gravitational waves and neutrinos [6, 7].

Because of the complexity of the problem, the modeling of the physical processes is still in evolution, but it is generally accepted that the role of neutrinos is critical for the energy transport as first suggested in [8]. The

collapse and the formation of a compact object, like a neutron star, have to pass through substantial neutrino emission, see, e.g., [9]. The details of how the explosion takes place and how the neutrinos are emitted are less clear and necessarily model dependent. In this work we focus on the only mechanism that has been studied in some detail: the *neutrino-driven mechanism* also known as Bethe and Wilson scenario [10] or delayed scenario for the explosion. In the neutrino-driven mechanism, the explosion of the massive star receives crucial assistance from the energy deposition due to an initial, intense neutrino luminosity. Although the viability of this mechanism cannot be considered fully demonstrated at present¹, recent theoretical results [12, 13] encourage the opinion that the neutrino-driven mechanism works for certain core collapse SN.

In the neutrino-driven mechanism, there are two main phases of neutrino emission:

- i) A thermal phase, called *cooling*, occurring when the proto-neutron star cools quietly. This phase involves most of the emitted neutrinos, 80-90% in energy.
- ii) A brief and very luminous neutrino emission, here termed *accretion*, that should involve a lower amount of neutrinos, 10-20% in energy. The accretion phase characterizes the neutrino-driven mechanism of the explosion, and it is expected to occur in the first stage of neutrino emission. In this phase, the matter is rapidly accreting over the proto-neutron star through the stalled super-

*Electronic address: giulia.pagliaroli@lngs.infn.it

†Electronic address: francesco.vissani@lngs.infn.it

‡Electronic address: marialaura.costantini@lngs.infn.it

§Electronic address: aldo.ianni@lngs.infn.it

¹ We note that relevant discussion can be traced back to 1978 with the calculations of Nadyozhin [11].

nova shock wave. The two most important processes of neutrino emission are

$$e^- p \rightarrow n \nu_e \text{ and } e^+ n \rightarrow p \bar{\nu}_e \quad (1)$$

due to the abundant presence of nucleons and of quasi-thermal e^+e^- plasma. These types of neutrinos (ν_e and $\bar{\nu}_e$) transfer to the star a small fraction of their energy, $f \sim 0.1$, necessary to revive the stalled shock wave. See [14] for a wide description of the phase of accretion, enriched by analytical arguments.

The neutrinos from phases *i*) and *ii*) can be observed in conventional supernova neutrino detectors [15] (namely, water Cherenkov and scintillators). In particular electron antineutrinos give signal mainly through inverse beta decay reaction on free protons:

$$\bar{\nu}_e p \rightarrow e^+ n \quad (2)$$

Thus the existence of the accretion and cooling phases, generically expected in the neutrino-driven scenario, can be experimentally verified.

B. What can we learn from SN1987A observations?

SN1987A is the first and the only occasion at present to test the credibility of the various hypotheses on how a SN works. In fact, the events observed by IMB [16, 17], Kamiokande-II [18, 19] and Baksan [20], represent a historic opportunity to investigate the physics of the collapse and of the explosion. A very extensive literature testifies the effort to extract information from these data with a wide variety of methods [21, 22, 23, 24, 25, 26, 27, 28, 29, 30, 31, 32, 33, 34, 35, 36, 37, 38, 39, 40, 41, 42, 43, 44]. Usually, a specific characteristic of the SN1987A data is studied, most frequently the energy distribution. The energy and the time distributions are jointly considered in a few analyses, but most often describing the neutrino emission with (overly) simple models, a procedure that is only partially justified by the limited amount of events collected.

The next neutrino observation will be an extraordinary occasion to progress, but recall that SN are rare on human time scale and it is not possible to reliably predict when the next one will happen. Thus, we should try our best using the only data that we have at our disposal, and in particular, we should attempt to address the question on *whether there is a hint of accretion from SN1987A observations*, as expected. In this respect, a point that deserves to be stressed is that all detectors observed a relatively large number of events in the first second of data taking, about 40 %: there are in fact 6 events in Kamiokande-II, 3 events in IMB and 2 events in Baksan.

A milestone for the point of discussion and more in general for SN1987A data analysis is the paper of Lamb and Loredó [36] (LL in the following), where it is argued that the SN1987A observations can be used to claim for an evidence of the accretion phase. The LL paper, widely

cited in theoretical and experimental reviews, is generally considered a useful application of refined statistical techniques and, in the present paper, we will provide the first independent verification of their results. However, we deem that, in view of the importance of their claim and in the light of various advances in neutrino physics (e.g., in oscillations, [47, 48, 49, 50] and [51, 52, 53, 54, 55]), it is necessary to offer a critical discussion of the assumptions of the analysis by Lamb and Loredó. More specifically:

- 1) the likelihood structure can be enhanced including a more accurate detection cross section [56], the information on the directions of the events, a different treatment of the background [44];
- 2) the theoretical model for neutrino emission, required for the data analysis, can be improved and approached as much as possible to the real signal expected from the numerical simulations of neutrino emission. In this respect, a specific criticism was raised by Raffelt and Mirizzi [42], who emphasized that the two-phase parameterization used in LL analysis leads to a sudden jump of the average neutrino energy while passing from accretion to cooling. This behavior is rather different from the expectations of the numerical simulations.

In short, our main tasks are to present a somewhat different likelihood, to propose an improved parameterization for neutrino flux, to include oscillations, and finally to evaluate the impact of the various new points for the analysis of SN1987A observations.

C. Layout of the work

The structure of this paper is the following: in Sect. II we discuss the construction of the likelihood function involved in the analysis of the data set, underlining the improvements carried in the description of detection rate; in Sect. III we propose a new parameterization for neutrino emission, building it step by step and discussing its features, leaving the description of certain technical details to the appendix; finally in Sect. IV we draw the results of our analysis.

II. LIKELIHOOD CONSTRUCTION

In this section we describe the likelihood that we adopted to compare the observed events and the assumed flux for the neutrino emission, stressing the novelties and the technical improvements.

A. Signal rate

The signal in each detector, triply differential in time, positron energy E_e and cosine of the angle θ between the

antineutrino and the positron is:

$$R(t, E_e, \cos \theta) = N_p \frac{d\sigma_{\bar{\nu}_e p}}{d\cos \theta}(E_\nu, \cos \theta) \Phi_{\bar{\nu}_e}(t, E_\nu) \times \xi_d(\cos \theta) \eta_d(E_e) \frac{dE_\nu}{dE_e}, \quad (3)$$

where N_p is the number of targets (=free protons) in the detectors, $\sigma_{\bar{\nu}_e p}$ is the inverse beta decay cross section (Eq. 2), η_d the detector dependent average detection efficiency, ξ_d is the angular bias =1 for Kamiokande-II and Baksan whereas for IMB $\xi_d(\cos \theta) = 1 + 0.1 \cos \theta$ [17], and, finally, $\Phi_{\bar{\nu}_e}$ is the electron antineutrino flux, differential in the antineutrino energy E_ν and discussed later in this work.

The expected number of signal events μ_s is the crucial ingredient, along with the expected number of background events μ_b , to construct the Poisson likelihood $\mu^n \exp(-\mu)/n!$, where $\mu = \mu_s + \mu_b$ and where n is the number of observed events. To evaluate μ_s we use Eq. 3: the number of expected signals in a bin is just $R(t, E_e, \cos \theta) dt dE_e d\cos \theta$; the total number of the events is the integral of $R(t, E_e, \cos \theta)$ over its three variables.

As mentioned in the introduction, our analysis is similar to the one of Lamb and Loredó [36], with whom we agree within errors when we strictly stick to their procedure. The signal rate that we adopted in this paper departs from their one in the following points:

1. Cross section and event direction

We adopt the inverse beta decay cross section calculated in [56] and in particular we use the differential expression $d\sigma_{\bar{\nu}_e p}/d\cos \theta$ given in Eq. (20) of that paper. The energy of antineutrino is given in terms of the positron energy E_e and of the angle θ between the antineutrino and the positron directions:

$$E_\nu = \frac{E_e + \delta_-}{1 - (E_e - p_e \cos \theta)/m_p}, \quad (4)$$

where $\delta_- = (m_n^2 - m_p^2 - m_e^2)/(2m_p) = 1.294$ MeV and p_e is the positron momentum. The new total cross section agrees at 10 MeV with the one used by Lamb and Loredó, whereas at 20 MeV (30 MeV) it is 6% (12%) smaller.

2. Efficiency

Following the traditional approach and differently from [36] we include in Eq. 3 the detection efficiency as a function of the true energy of the event. A formal justification of our procedure is given in [46], that is in contrast with the formal justification in Appendix A of [36].

Our procedure simply accounts for the evident fact that the expected number of *signal* events μ_s should include all relevant detector dependent features: loss of

events due to light attenuation, fluctuations of the number of photoelectrons, detector geometry, *etc.*. These features produce an imperfect ($\eta_d < 100\%$) detection efficiency, that means that only a fraction of the produced positrons is actually detected. We have in mind an *average efficiency* evaluated by a MC procedure, namely 1) simulating several events with true energy E_e but located in the various positions and emitted in all possible directions, then 2) counting the fraction of times that an event is recorded, finally 3) deducing also the ‘smearing’ (=average error as a function of E_e).

It is possible to argue in favor of our procedure by considering the following situation. Imagine two detectors that differ by the detector efficiency: $\eta = 100\%$ in the first one, $\eta = 10\%$ in the second, and with a rate of positron production equal to the background rate. Suppose that each of these detectors observed one event. According to the procedure of [36] (used, e.g., to obtain their Tab. VI) the probability that the observed event is due to a signal is 50% in both detectors, that we find paradoxical: the better the detector, the higher should be the chances of a signal. Instead, adopting our procedure, the probability that the event is due to a signal is 50% in the first detector and 9% in the second one, which we find more plausible.

We recall (in agreement with [36, 44]) that for an even more refined analysis of the data, one should not use the average detection efficiency, but should rather evaluate the specific detection efficiency and background rate for any individual event. In our understanding, a correction on individual basis of this type was performed only to assess the errors on the energies of the events, see [19].

B. The assumed likelihood

We estimate the theoretical parameters by the χ^2 :

$$\chi^2 \equiv -2 \sum_{d=k,i,b} \log(\mathcal{L}_d), \quad (5)$$

where \mathcal{L}_d is the likelihood of any detector (k, i, b are shorthands for Kamiokande-II, IMB, Baksan). We use Poisson statistics; dropping constant (irrelevant) factors, the ‘unbinned’ likelihood of each of the 3 detectors is:

$$\mathcal{L}_d = e^{-f_d \int R(t) dt} \times \prod_{i=1}^{N_d} e^{R(t_i) \tau_d} \times \left[\frac{B_i}{2} + \int R(t_i, E_e, \cos \theta_i) \mathcal{L}_i(E_e) dE_e \right]. \quad (6)$$

We denote by $R(t)$ the integral of $R(t, E_e, \cos \theta)$ over the variables E_e and $\cos \theta$. In IMB, the live-time fraction is $f_d = 0.9055$ and the dead-time is $\tau_d = 0.035$ s, whereas for the other detectors $f_d = 1$ and $\tau_d = 0$. Each detector saw N_d events; their time, energy and cosine with supernova direction are called t_i , E_i and c_i ($i = 1 \dots N_d$).

\mathcal{L}_i is a Gaussian distribution that includes the estimated values of the energy E_i and the error of the energy δE_i for each individual event, accounting for the

detector-dependent effects on energy measurements. The inclusion of the error on the measurement of $\cos\theta$ does not change significantly the likelihood, so we simply set $\cos\theta = c_i$ for each event.² Finally, we do not include an error on the event times δt_i , since the relative time of each event is precisely measured.

The absolute times have not been measured precisely enough (except for IMB). However, the procedure of analysis that we adopt requires only the relative times between the events: the experimental input is $\delta t_i = t_i^{\text{exp}} - t_1^{\text{exp}}$. The times t_i are defined as follows:

$$t_i = t^{\text{off}} + \delta t_i \quad (7)$$

where $t^{\text{off}} \geq 0$ is the offset (or delay) time between the first neutrino that reached the Earth (that, by definition, occurred at $t = 0$) and the first event that was detected. We introduce one parameter t^{off} for each detector, and fit their values from the data. The integral over the time in the first exponential factor of Eq. 6 is performed from the moment when the first neutrino reaches the Earth till the end of data taking, $t = 30$ s; the condition that all the data are included imposes mild restrictions, such as $t_{\text{KII}}^{\text{off}} < 6$ s, that do not have a relevant role in the analysis.

1. Background

The probability that an event is due to background is denoted by B_i in Eq. 6. It is calculated as $B_i = B(E_i)$: B_i is the *measured* background rate for the given energy [Hz/MeV]. The background distribution differential in time, energy and cosine is $B(E_e)/2$; the factor $1/2$ describes a uniform cosine distribution. This definition is different from the one of LL, $B_i = \int B(E_e) \mathcal{L}_i(E_e) dE_e$, that has been argued to be inaccurate in [44]. The values of B_i that we use for Kamiokande-II are given in Appendix A of [44]. The events of Kamiokande below 7 MeV have a higher background rate than found by LL, those above 9 MeV a lower background rate, while the other ones stay almost unchanged. The changes for Baksan are instead negligible. It is fair to assume in good approximation that, in the time window of interest, IMB observations are safe against background contamination.

III. ANTINEUTRINO FLUX DESCRIPTION

In this section we describe the parameterization of the neutrino flux that we adopt. We describe the signal introducing three ‘microscopic’ (i.e., physically meaningful) parameters for each phase, that, roughly speaking,

are needed to quantify the duration of the emission process, the intensity of the emission and the average energy of the antineutrinos. The adopted time distributions are constructed to enforce the continuity of the instantaneous luminosity and of the average energy as found in the numerical simulations. Moreover, we tried to maintain the parameterization as simple as possible.

A. Parameterized antineutrino fluxes

1. Cooling phase

In the last phase of the SN collapse the nascent proto-neutron star evolves in a hot neutron star (with radius R_{ns}) and this process is characterized by a neutrinos and antineutrinos flux of all species. This is the *cooling* phase; we use the suffix *c* in the corresponding symbols.

A rather conventional parameterization of the electron antineutrino flux, differential in the energy is:

$$\Phi_c^0(t, E_\nu) = \frac{1}{4\pi D^2} \frac{\pi c}{(hc)^3} [4\pi R_c^2 g_{\bar{\nu}_e}(E_\nu, T_c(t))] \quad (8)$$

where the Fermi-Dirac spectrum of the antineutrinos is

$$g_{\bar{\nu}_e}(E_\nu, T_c(t)) = \frac{E_\nu^2}{1 + \exp[E_\nu/T_c(t)]} \quad (9)$$

The time scale of the process is included in the function:

$$T_c(t) = T_c \exp[-t/(4\tau_c)]. \quad (10)$$

Eq. 8 describes an isotropic emission of antineutrinos from a distance $D (= 50$ kpc in the case of SN1987A). [We use the symbol Φ^0 rather than Φ to emphasize that flavor oscillations have not been included yet].

The astrophysical free parameters are R_c , T_c , and τ_c namely: the radius of the emitting region (neutrino sphere), the initial temperature, and the time constant of the process. We recall which are the generic expectations: $R_c \sim R_{ns} = 10 - 20$ km, $T_c = 3 - 6$ MeV, and $\tau_c = \text{few-many seconds}$. Rather than using these *a priori*, we will deduce the value of these parameters by fitting the SN1987A data, and later, we will compare the results with the expectations.

2. Accretion phase

After the bounce, the simulations indicate that the shock wave, propagating into the outer core of the star, loses energy and eventually gets stalled. It forms an accreting shock that encloses a region of dissociated matter and hot e^+e^- plasma, where the weak reactions of Eq. 1 give rise to intense ν_e and $\bar{\nu}_e$ luminosities. This emission lasts a fraction of a second. In the Appendix we describe in more details the conceptual scheme for $\bar{\nu}_e$ emission: a neutron target exposed to a flux of thermal

² For the first 12 Kamiokande-II and for the 8 IMB events the value of $\cos\theta = c_i$ is measured; we set instead $c_i = 0$ for the 5 events of Baksan and the last 4 events (out of 16) of Kamiokande-II.

positrons. The neutrons are treated as a transparent target, for only a small fraction of antineutrinos is expected to couple with the star. This is the *accretion* phase; we use the suffix *a* in the corresponding symbols.

The parameterized $\bar{\nu}_e$ flux is

$$\Phi_a^0(t, E_\nu) = \frac{1}{4\pi D^2} \frac{8\pi c}{(hc)^3} \times [N_n(t) \sigma_{e^+n}(E_\nu) g_{e^+}(\bar{E}_{e^+}(E_\nu), T_a(t))], \quad (11)$$

where $N_n(t)$ is the number of target neutrons assumed to be at rest and the thermal flux of positrons:

$$g_{e^+}(E_{e^+}, T_a(t)) = \frac{E_{e^+}^2}{1 + \exp[E_{e^+}/T_a(t)]} \quad (12)$$

is calculated at an average positron energy, namely $\bar{E}_{e^+}(E_\nu) = \frac{E_\nu - 1.293 \text{ MeV}}{1 - E_\nu/m_n}$. In the energy range of interest, $E_\nu = 5 - 40$ MeV, a simple numerical approximation of the cross section for positron interactions is

$$\sigma_{e^+n}(E_\nu) \approx \frac{4.8 \times 10^{-44} E_\nu^2}{1 + E_\nu/(260 \text{ MeV})} \quad (13)$$

The derivation of Eqs. 11 and 13 is given in the appendix.

The average energy of the antineutrinos is roughly given by $5 T_a$ and the spectrum is slightly non-thermal,³ mostly due to the presence of the cross section σ_{e^+n} . For example, when $T_a = 1.5, 2.5, 3.5$ MeV, we get $\langle E_\nu \rangle / T_a = 5.5, 5.2, 5.0$ respectively and $\delta E_\nu / T_a = 0.39, 0.41, 0.41$ where $\delta E_\nu \equiv \sqrt{\langle E_\nu^2 \rangle - \langle E_\nu \rangle^2}$. Another manifestation that the distribution is non-thermal is the scaling of the luminosity with the temperature, roughly as T_a^6 —different from the thermal scaling T_a^4 . In order to give some feeling of the antineutrino emission, if we suppose that at $t = 0$ we have $T_a = 2.5$ MeV and $M_a = 0.15 M_\odot$ (see just below for a precise definition of these quantities) we get a luminosity of 1.1×10^{53} erg/s; the same luminosity and average energy would be given by a black body distribution with $T_c = 4.1$ MeV and $R_c = 82$ km.

There are two time dependent quantities in Eq. 11: the number of neutrons $N_n(t)$ and the positron temperature $T_a(t)$. It is straightforward to introduce a temperature that interpolates from an initial value to a final value:

$$T_a(t) = T_i + (T_f - T_i) \left(\frac{t}{\tau_a} \right)^m \text{ with } \begin{cases} T_i = T_a \\ T_f = 0.6 T_c \end{cases} \quad (14)$$

where T_a denotes the *positron* temperature at the beginning of accretion (to be contrasted with T_c , the *antineutrino* temperature at the beginning of the cooling phase). With this parametrization, the positron temperature reaches $0.6 T_c$ at $t = \tau_a$, that is what is needed

match the average antineutrino energies, namely, to ensure a continuous behavior of the average antineutrino energy (in particular at the end of the accretion phase and at the beginning of the cooling phase). The power $m = 1 - 2$ mimics the behavior found in numerical simulations; we adopt $m = 2$ as a default value.

Now we discuss the time evolution of the number of neutrons exposed to positrons $N_n(t)$, proportional to the luminosity in accretion. Our goal would be a luminosity that, at least for $t \sim 0$, decreases as $1/(1 + t/0.5 \text{ s})$. This behavior is suggested by the numerical simulations and is advocated by LL [36]. However, when we allow the temperature to vary, we vary also the luminosity, that scales as $N_n T_a^6$. Thus, we need to include an explicit factor $(T_a(t)/T_a)^6$. We arrive at our prescription for the number of neutrons exposed to thermal positrons:

$$N_n(t) = \frac{Y_n}{m_n} \times M_a \times \left(\frac{T_a}{T_a(t)} \right)^6 \times \frac{j_k(t)}{1 + t/0.5 \text{ s}}, \quad (15)$$

the fraction of neutrons being set to $Y_n = 0.6$. M_a is the initial accreting mass exposed to the positrons thermal flux. The time-dependent factor

$$j_k(t) = \exp[-(t/\tau_a)^k], \quad (16)$$

is included to terminate the accretion phase at $t \sim \tau_a$. LL use $k = 10$, which however leads to a very sharp drop of the luminosity at $t \sim \tau_a$. In our calculations, we will set instead $k = 2$, a choice that offers the advantage of leading to a smooth (reasonable, continuous) luminosity curve, closer to the type of curves found in numerical simulations. [We will show in the next section luminosity curves with $k = 10$ and with $k = 2$.]

Ultimately, the accretion phase involves 3 free parameters: M_a and T_a and τ_a , the same number of parameters of the cooling phase. Finally, we give rather generic expectations on values of these parameters: M_a is certainly lower than the whole outer core mass (about $0.6 M_\odot$); T_a is expected to sit in the few MeV range; and, finally, the accretion should last a fraction of a second, $\tau_a \sim 0.5$ s being a typical number.

B. Temporal shift

In the model advocated by Lamb and Loredó and adopted for the analysis of SN1987A data, the accretion and the cooling phases are contemporaneous. This has the consequence that for times $t < \tau_a$, the antineutrino distribution is not a thermal spectrum, but a composition (=sum) of two thermal spectra, whose average energies differ by more than a factor of 2 in the best-fit point. At low energies, the spectrum is dominated by the antineutrinos from accretion; at the highest energies, by the antineutrinos from cooling. The possibility to have a *composite spectrum* implies, among the other things, that it is easy (trivial) to reconcile the low energy events observed by Kamiokande-II and the high energy events

³ The deviation from the thermal distribution can be described by a ‘pinching factor’—an *effective* chemical potential introduced to distort the Fermi-Dirac thermal spectrum—in the range 4-5, that decreases when T_a increases; e.g., for $\delta E_\nu / T_a = 0.41$ the pinching factor is 4.2.

observed by IMB in the first second: they simply belong to different and simultaneous phases of emission. We will verify this statement later by a straightforward calculation—see Tab. II. We note in passing that such a composite spectrum is used in the work of Loredano and Lamb [36] but this characteristic feature is neither commented or discussed there. The compositeness of the LL spectrum (i.e., the non-thermal tail) can be better perceived plotting it in logarithmic scale and/or by considering the time-integrated spectrum, see Fig. 2 of [45].

However, at the best of our knowledge there is no evidence from numerical simulations of a composite behavior of the spectrum; the instantaneous $\bar{\nu}_e$ spectrum is found to be quasi-thermal at any time and typically this property is shared also by the time-integrated spectrum; see, e.g., the discussions in [57, 58, 59]. Deviations from a thermal distribution are observed, especially during accretion [29, 60, 78]; they can be effectively described by a ‘pinching’ parameter of the order of a few, that means that the high-energy tail of the spectrum is depleted—not enhanced as for the composite model advocated by LL.

In short, we believe that, in absence of an explicit indication from numerical simulations, the model that should be adopted in data analyses (and/or the null-hypothesis that should be tested) is the simplest one compatible with the numerical simulations, namely: a $\bar{\nu}_e$ spectrum quasi-thermal at any time—rather than, e.g., ‘composite’ [36], bimodal [43] or exponentially decreasing in the energy [42]. For this reason, we parameterize the antineutrino flux as follows:

$$\Phi_{\bar{\nu}_e}(t) = \Phi_a(t) + (1 - j_k(t)) \times \Phi_c(t - \tau_a). \quad (17)$$

where Φ_a (resp., Φ_c) is given in Eq. 11 (resp., Eq. 8) in the case when oscillations are absent. Recalling that $j_k(t)$ appears explicitly in Eq. 15, i.e., in the accretion flux, it is clear that the effect of this function is simply to interpolate between the two phases of neutrino emission; in other words, the cooling phase begins around $t = \tau_a$.

We note here a limit in which the likelihood becomes unphysical. Consider the case when only the first event detected by Kamiokande-II falls in the accretion phase. If the accretion were to last a very short amount of time, $\tau_a \ll \delta t_2$, and if $t^{\text{off}} \ll \delta t_2 = 0.107$ s, the antineutrino flux at the time of the first event $t = \delta t_1 = 0$ could become very large even if the number of expected number of events remains small. In this limit, the interaction rate in Eq. 3 becomes large, too. Thus, due to the factor $R(t_1, E_e, \cos \theta_1)$ in Eq. 6, the likelihood can be made arbitrarily large, because the exponential factor in the same equation (that depends on the expected number of events) will not change much. The way to avoid this pitfall is to require a lower limit on τ_a in the numerical calculations. A limit that is adequate for the analysis of data from SN1987A is $\tau_a > 0.3$ s. We will demonstrate explicitly the presence of this unphysical behavior of the likelihood function later, when discussing its maxima.

C. Neutrino oscillations

Here we discuss the effects of neutrino oscillations on the observed $\bar{\nu}_e$ fluxes. The survival probability P for $\bar{\nu}_e$ emitted by supernova is dictated by two different interactions with the star medium. The first is the usual matter effect [57, 61] of charged current interactions between $\bar{\nu}_e$ and the electrons of the matter. The second is the effect of $\nu - \nu$ interactions [62, 63, 64, 65, 66], that is known to be important in specific cases [67, 68] and whose behavior has been quantified in certain approximations [69, 70, 71, 72]. In order to describe oscillations we have to distinguish the two arrangements of the neutrino mass spectrum that are compatible with the present knowledge of neutrino properties (see, e.g., [75]): For **normal** mass hierarchy the survival probability and the observed $\bar{\nu}_e$ flux are:

$$P = U_{e1}^2, \quad (18)$$

$$\Phi_{\bar{\nu}_e} = P \Phi_{\bar{\nu}_e}^0 + (1 - P) \Phi_{\bar{\nu}_\mu}^0,$$

where we recall that Φ^0 is the flux in absence of oscillations. We have assumed that $\Phi_{\bar{\nu}_\mu}^0 = \Phi_{\bar{\nu}_\tau}^0$ and each term is the sum of the cooling flux and accretion flux. The $\nu - \nu$ interaction is most relevant for **inverted** mass hierarchy [69, 70, 71, 72, 73, 74]. As an example the electron antineutrino survival probability given in [72] is:

$$P = U_{e1}^2(1 - P_f) + U_{e3}^2 P_f, \quad (19)$$

$$\Phi_{\bar{\nu}_e} = P \Phi_{\bar{\nu}_e}^0 + (1 - P) \Phi_{\bar{\nu}_\mu}^0.$$

We adopt the usual decomposition of the mixing elements in terms of the mixing angles: $U_{e3} = \sin \theta_{13}$ and $U_{e1} = \cos \theta_{12} \cos \theta_{13}$ with $\theta_{12} = 35^\circ \pm 4^\circ$ and $\theta_{13} < 10^\circ$ at 99 % C.L. For the measured solar oscillation parameters, the Earth matter effect is known to be small (see, e.g., [76]). We include it in the analysis anyway evaluating the survival probabilities with the PREM model [77]. In the case of normal mass hierarchy the probability $P \sim 0.7$ is reliably predicted and rather precisely known. Instead, for inverted mass hierarchy, P depends strongly on the unknown mixing angle θ_{13} . In fact, the flip probability P_f (that quantifies the loss of adiabaticity at the ‘resonance’ related to the atmospheric Δm^2) is:

$$P_f(E_\nu, \theta_{13}) = \exp \left[-\frac{U_{e3}^2}{3.5 \times 10^{-5}} \left(\frac{20 \text{ MeV}}{E_\nu} \right)^{2/3} \right], \quad (20)$$

where the numerical value corresponds to the supernova profile $N_e \sim 1/r^3$ given in [61]. The predictions for the $\bar{\nu}_e$ flux in the detector could be tested with a relatively large amount of data: a galactic supernova could turn out to be useful to discriminate the right mass hierarchy.

We assume that an equal amount of energy goes in each species (equipartition hypothesis) during cooling. Furthermore, we suppose that the temperature of $\bar{\nu}_\mu$ and $\bar{\nu}_\tau$ is in a fixed ratio with the $\bar{\nu}_e$ temperature. Following [78]

we assume:

$$T(\bar{\nu}_\tau)/T(\bar{\nu}_e) = T(\bar{\nu}_\mu)/T(\bar{\nu}_e) = 1.2, \quad (21)$$

We tested that a value in the 1.0-1.5 or a deviation of the amount of energy stored in non-electronic neutrino species by a factor of 2 does not affect crucially the fitted antineutrino flux. In the accretion phase, we will suppose that only ν_e and $\bar{\nu}_e$ are emitted in equal amount, whereas $\Phi_a^0(\bar{\nu}_x) = 0$. The fit provides a reasonably fair description of the antineutrino flux anyway, but the estimation of the amount of energy emitted during accretion should be considered as a lower bound.

IV. RESULTS

In the previous two sections we constructed, step by step, a likelihood function that represents the probability function of the overall data set. This probability varies in the parameters space and depends on the model for the antineutrino emission. As anticipated, the main goal of this paper is to verify if the best-fit values of the parameters, that maximize the likelihood function, are physically acceptable.

We remark that LL adopted a Bayesian analysis while we use a frequentist approach, which occasionally leads to some difference in the confidence levels, but not in the best fit points. More specifically to calculate the error on one parameter we use as a rule the profile likelihood, namely the likelihood evaluated fixing the parameter of interest and maximizing the other (nuisance) parameters. A similar procedure allows us to calculate the confidence regions.

The structure of this section is the following: in Sect. IV A we describe the simpler (one component) model, in Sect. IV B we describe the more complete (two components) model. This second part illustrates the impact of each improvement in the description of the flux; the final result is discussed in detail in Sect. IV B 5.

A. One component model

Here we list the results of the likelihood maximization procedure when we include only the cooling phase. This model has 6 parameters: the $\bar{\nu}_e$ temperature T_c , the duration τ_c , the neutrinosphere radius R_c and the three detector offset times t^{off} . It is identical to the “Exponential cooling model” reported in [36], also termed “minimum” or “standard” model in [27]. The comparison of the best-fit values of LL ($R_c = 40$ km, $T_c = 3.81$ MeV, $\tau_c = 4.37$ s and $t^{\text{off}} = 0$ s [36]) with our results ($R_c = 44$ km, $T_c = 3.68$ MeV, $\tau_c = 4.43$ s and $t^{\text{off}} = 0$ s) is satisfactory, the agreement being at the level of 10%.

We proceed and quantify the impact of the improvements in the likelihood described in Sect. II. The inclusion of the detection efficiency $\eta(E_{e+})$ gives the

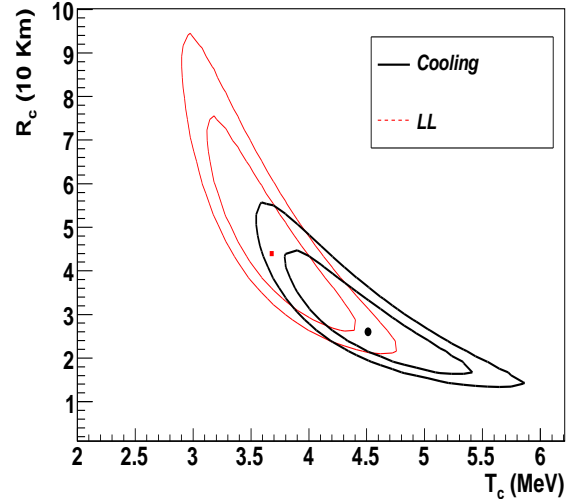


FIG. 1: Two dimensional confidence regions for the cooling parameters R_c and T_c . The gray (red) contours are the exponential cooling result (68% and 90% C.L.) following Lored and Lamb analysis. The dark contours are our result for one component cooling model. The best fit points are also displayed.

single most important effect. In fact we obtain:

$$R_c = 30 \text{ km}, T_c = 4.21 \text{ MeV}, \tau_c = 3.88 \text{ s}. \quad (22)$$

Using the new cross section $\sigma_{\bar{\nu}_e p}(E_{\nu_e})$ for the inverse beta decay we get the new best-fit point values:

$$R_c = 26 \text{ km}, T_c = 4.58 \text{ MeV}, \tau_c = 3.72 \text{ s}. \quad (23)$$

Our assumption on the background B_i has a little effect on these values that become $R_c = 26$ km, $T_c = 4.59$ MeV and $\tau_c = 3.81$ s.

Similarly the inclusion of the event directions, $\cos\theta_i$ (Eq. (20) in [56]), that produces:

$$R_c = 26 \text{ km}, T_c = 4.47 \text{ MeV}, \tau_c = 3.88 \text{ s}. \quad (24)$$

The values of t^{off} parameters are always zero in these models, and it is easy to convince oneself that this is due to the fact that, in this one component model, the signal is forced to decrease with the time.

The larger change concerns the radius R_c that diminishes by 35% in comparison to the value given by Lamb and Lored, approaching the expected neutron star radius, but still twice larger than a typical value. In Fig. 1 we show the contour plots in the $R_c - T_c$ plane, the two parameters that show the largest correlation among them. In gray we draw the 68% and 90% contours level that we obtain adopting the same likelihood function of LL, in black the contours level when we construct the likelihood function following Sec. II, i.e., including all the structural improvements discussed above.

With the best-fit points it is possible to estimate the total energy emitted by neutrinos in this model. Hypothesizing that in the cooling phase all types of neutrinos are emitted, each one carrying away an equal amount of energy, the total energy is:

$$\frac{E_c}{10^{53}\text{erg}} = 3.39 \times 10^{-6} \int_0^\infty dt \left(\frac{R_c}{\text{km}} \right)^2 \left(\frac{T_c(t)}{\text{MeV}} \right)^4, \quad (25)$$

This value should be comparable with the gravitational binding energy of the new born neutron star, $E_b = (1-5) \cdot 10^{53}$ erg. The LL result for exponential cooling model is $E_b = 5.02 \cdot 10^{53}$ erg, namely a binding energy at the upper limit of this range, whereas our results $E_b = 3.55 \cdot 10^{53}$ erg is included in the expected range.

B. Two components model

Now we include both emission phases. Following the order of Sect. III, we improve, step by step, the emission model of the accretion phase. To describe accretion we add 3 new physical parameters, namely: the positrons temperature T_a , the duration of the accretion phase τ_a and the initial accreting mass M_a . So the likelihood is a function of 9 parameters. The best fit results are given in table I and will be commented in details below.

The last column of Tab. I shows the values $\Delta\chi^2 = \chi_c^2 - \chi_m^2$, where χ_c^2 is calculated with the best one-component model of the previous section, i.e., the last case of previous subsection (eq. 24), and χ_m^2 is calculated with the model described in the section indicated in each line of Tab. I. The larger the difference, the larger the evidence for accretion; a quantitative evaluation of the evidence, taking into account the increased number of parameters, is provided later.

1. Effect of the new likelihood-improvements of Sect. II

The first line of Tab. I shows the best-fit results obtained using the likelihood function constructed in our Sect. II and one of the emission model used by LL, namely the model called ‘‘Exponential cooling and truncated accretion’’ (later called ECTA) [36]. We see that the best-fit value for the initial accreting mass M_a is very large and hardly acceptable on physical basis: this parameter is restricted by $M_a < 0.6 M_\odot$ for the reasons mentioned in Sect. III A 2. This result, however, is in agreement with what found by Lamb and Loredo, who fixed $M_a \equiv 0.5 M_\odot$ in all models of their table V, namely they inserted a ‘‘prior’’ in their analysis. This assumption reduces to 8 the number of free parameters and produces these best-fit values:

$$R_c = 12 \text{ km}, \quad T_c = 5.40 \text{ MeV}, \quad \tau_c = 4.40 \text{ s}, \quad (26)$$

$$M_a \equiv 0.5 M_\odot, \quad T_a = 2.02 \text{ MeV}, \quad \tau_a = 0.70 \text{ s}$$

with $\Delta\chi^2 = 13.4$. We call this best-fit point LL^* to distinguish it by the true global maximum of likelihood

Sect.	R_c [km]	T_c [MeV]	τ_c [s]	M_a [M_\odot]	T_a [MeV]	τ_a [s]	$t_{\text{off}}^{\text{off}}$ [s]	$\Delta\chi^2$
II	12	5.46	4.25	5.59	1.52	0.72	0.	14.7
III A	14	4.99	4.76	0.82	1.75	0.67	0.	11.2
III B	14	4.88	4.72	0.14	2.37	0.58	0.	9.8
III C	16	4.62	4.65	0.22	2.35	0.55	0.	9.8

TABLE I: *The best-fit values of the astrophysical parameters for two components model neutrino emission. Each line of this table is an incremental step toward the final improved parameterization. The last column shows the difference between the χ^2 of our one-component (cooling) model and the χ^2 of each two-component model.*

function, shown in Tab. I. In passing, we note that our modifications of the likelihood do not really change the conclusions of Lamb and Loredo [79].

2. New spectrum and $T_a(t)$ -improvements of Sect. III A

The second line of table I shows that there is less need of the *a priori* on M_a when we exploit the correct parametrization of the accretion flux (accounting for the right kinematics of e^+n process, using the new cross section and allowing the positron temperature to increase with the time). In fact the best fit value for the initial accreting mass decreases to $M_a = 0.82 M_\odot$ in this model, a value that is a bit larger than the reference outer core mass, $0.6 M_\odot$, but now closer to the expected range. The accretion phase is characterized by a low mean energy and by a duration shorter than a second, as expected. The total energy carried in each phase is: $E_c = 2.0 \cdot 10^{53}$ erg and $E_a = 5.7 \cdot 10^{52}$ erg, and the total binding energy is $E_b = E_a + E_c = 2.5 \cdot 10^{53}$ erg. It is important to note that, in this model and as in the LL model (see Sect. III B) the two emission phases are contemporaneous. This implies that the emission spectrum is ‘‘composite’’, a features that makes it easier to account for the difference between the average energies of IMB and of Kamiokande-II, as can be seen from the relatively high value of $\Delta\chi^2$ in table I.

3. Separating accretion and cooling-improvements of Sect. III B

In Sect. III B we discussed a procedure (‘‘time shift’’) to separate temporally the accretion and cooling phases. The time shift produces two families of best fit values: when the IMB data fall in the accretion phase ($t_{\text{IMB}}^{\text{off}} \sim 0$) the positron temperature T_a has to increase; when the IMB data fall in the cooling phase ($t_{\text{IMB}}^{\text{off}} \sim \tau_a$) the temperature T_a can remain relatively low. We show in Fig. 2 the likelihood profile of T_a parameter, where the

above situation becomes evident.⁴ The figure refers to final model that includes also neutrino oscillations, but the same structure arises already as soon as the time-shift is included. The other local maximum of the likelihood besides the one shown in Tab. I is at:

$$\begin{aligned} R_c &= 10 \text{ km}, & T_c &= 5.28 \text{ MeV}, & \tau_c &= 4.74 \text{ s}, \\ M_a &= 1.27 M_\odot, & T_a &= 1.65 \text{ MeV}, & \tau_a &= 1.4 \text{ s} \end{aligned} \quad (27)$$

with $t_{\text{IMB}}^{\text{off}} = 0.93 \text{ s}$ and $\Delta\chi^2 = 10.2$. The χ^2 values obtained with this best-fit solution is very near to best-fit value shown in Tab. I, the difference being only ~ -0.5 . Therefore this solution cannot be discarded on statistical basis. Thus, let us examine the physical content of this solution. When the data of IMB belong to cooling phase, as in this solution, the value of T_a diminishes to account for the mean energy of the first KII events, and the initial accreting mass M_a increases to achieve the right number of detected events. This implies that the family of solution with a temporal shift different from zero has larger values of M_a . The solution of Eq. 27 has a time constant τ_a two-three times larger than the expectations and, more importantly, it has a value M_a twice the outer core mass; instead, the solution of Tab. I has a completely acceptable value of M_a . Since we expect that only a fraction of the outer core mass is exposed to the thermal positron flux, we are led to believe that the latter solution is more plausible than the former.

4. Effects of oscillations–improvements of Sect. III C

In the last line of Tab. I, we complete the parameterization of the flux by including neutrino oscillations. The solution is very similar to the one described in the previous section and the astrophysical parameters are rather similar to the expectations. The total energy emitted by neutrinos in each emission phase is: $E_c = 1.8 \cdot 10^{53} \text{ erg}$ and $E_a = 4.8 \cdot 10^{52} \text{ erg}$ and the total binding energy is $E_b = 2.2 \cdot 10^{53} \text{ erg}$. The best-fit values have been obtained for normal hierarchy and with the assumptions discussed in Sect. III C. The flux of $\bar{\nu}_e$ that reaches the detectors is a combination of the $\bar{\nu}_e$ and $\bar{\nu}_\mu$ emitted within the star. The best-fit values showed in the table refers to the radius and temperature of $\bar{\nu}_e$, that however are closely related to the $\bar{\nu}_\mu$ values. In fact the temperature of emission is $T_c(\bar{\nu}_\mu) = 5.5 \text{ MeV}$ (due to Eq. 21) and the radius of $\bar{\nu}_\mu$ neutrinosphere is $R_c(\bar{\nu}_\mu) = 10 \text{ km}$ (due to equipartition).

The assumption that we can neglect the ν_μ during accretion implies that the accretion flux is suppressed by the factor $P = \cos^2 \theta_{12} \sim 0.7$, so the best-fit of initial

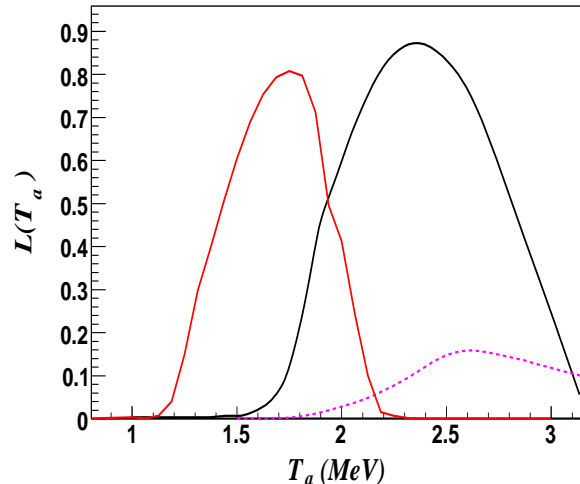


FIG. 2: Profiles likelihood for T_a parameter of accretion with the complete emission model (III.C). The red line is the family of solutions with $t_{\text{IMB}}^{\text{off}} \simeq 0.5 \text{ s}$. The dark line is the other family of solutions with $t_{\text{IMB}}^{\text{off}} = 0$ and $M_a < 1M_\odot$. The dotted line is the unphysical family of solutions discussed in Sect. III B with $\tau_a = 0.2 \text{ s}$.

accreting mass has to increase by $1/P$ to maintain the same fit. This quantitative change has some impact on the interpretation of the multiple solutions: In fact, the family of solutions with $t_{\text{IMB}}^{\text{off}} \neq 0 \text{ s}$ and with lower values T_a (red line of Fig. 2) turns out to be characterized by values of M_a greater than $1M_\odot$. Thus, physical considerations on the meaning of the accreting mass suggest, as more plausible, the family of solutions shown with a dark line in Fig. 2 and in the last line of Tab. I.

For inverted mass hierarchy, the effects of $\nu - \nu$ interactions are known to be relevant but their quantitative treatment is still under discussion, see e.g., [73, 74]. This consideration, already, prevents us to draw firm conclusions. However, adopting the formulae given in Sect. III C to illustrate which are the possible effects, we can distinguish 2 main cases: large values of θ_{13} , namely $\theta_{13} > 0.5^\circ$ and small values of θ_{13} , namely $\theta_{13} < 0.1^\circ$. In the first case, $P_f \sim 0$ and the survival probability $P = U_{e1}^2$; thus, we find the same results as for normal hierarchy. In the second case, the flip probability is $P_f \sim 1$ and $P = U_{e3}^2$ in Eq. 19. The suppression of the $\bar{\nu}_e$ survival probability $P \sim 0$, along with the assumption that the flux of $\bar{\nu}_\mu$ and $\bar{\nu}_\tau$ are very small during accretion, implies the *absence* of electron antineutrino events during accretion⁵. Such a hypothesis can be tested with–

⁴ In technical terms, the case when there are multiple maxima of similar quality is termed as pathological likelihood. The statistical concept of ‘pathological’ solution should be distinguished from the concept of ‘unphysical’ solution; e.g., the one corresponding to dotted line of Fig. 2 and explained in Sect. III B.

⁵ Note that neglecting $\nu - \nu$ interaction, the condition $P \sim 0$ turns out to be realized in the other case, namely for *large* values of θ_{13} [79].

and, to some extent, excluded by SN1987A observations [79]. All in all, the result for inverted hierarchy should be taken with great caution for it depends crucially not only on the present understanding of the effects of $\nu - \nu$ interactions but also on the incomplete description of the flux of $\bar{\nu}_\mu$ and $\bar{\nu}_\tau$ during accretion.

5. Remarks on the two component models

Having calculated the best fit values of the two component model, and having understood their meaning, we pass to discuss: (a) the evidence for the accretion phase (namely, we compare the two component and the one component model); (b) the errors on the best fit parameters for the improved model; (c) the difference between the best-fit ECTA model and our improved model.

a. Evidence for the phase of accretion In order to test whether the $\Delta\chi^2$ of the models with accretion (Tab. I) are just an effect of fluctuations, we perform a standard likelihood ratio significance test⁶ [80]. For the four models of table I, we find that we can reject the null hypothesis (=no accretion) with a significance level of $\alpha = 0.2\%$, $\alpha = 1.1\%$, and $\alpha = 2.0\%$ (for the last two models) respectively. Three remarks are in order:

(1) The result $\alpha = 0.2\%$ basically agrees with the claim of Lamb and Loredò: the ECTA model for emission, if correct, would lead to an important evidence for accretion. Our improvements in the likelihood (described in Sect. II) do not change this inference significantly.

(2) Also the other models permit to exclude the ‘null hypothesis’ that we test (namely, the absence of an accretion phase) with the conventional 5% criterion. But the evidence becomes a bit weaker and if one prefers to be very conservative, this could suggest caution. This outcome can be easily understood by the fact that our model for accretion is more constrained and can account for certain features of the data (such as the difference of IMB and KII energies) only at the price of some tension, that is reflected by the increased value of α .

(3) Obviously, even the conservative attitude does not forbid us to use the SN1987A data to learn something on accretion. It is the question that we formulate that changes: if we *assume* that the accretion phase exists, we can ask the data to determine the model parameters.

b. Errors on the parameters The 1σ errors obtained by a conventional, $\Delta\chi^2 = 1$, Gaussian procedure [80] are:

$$\begin{aligned} R_c &= 16_{-5}^{+9} \text{ km}, & M_a &= 0.22_{-0.15}^{+0.68} M_\odot, \\ T_c &= 4.6_{-0.6}^{+0.7} \text{ MeV}, & T_a &= 2.4_{-0.4}^{+0.6} \text{ MeV}, \\ \tau_c &= 4.7_{-1.2}^{+1.7} \text{ s}, & \tau_a &= 0.55_{-0.17}^{+0.58} \text{ s}. \end{aligned} \quad (28)$$

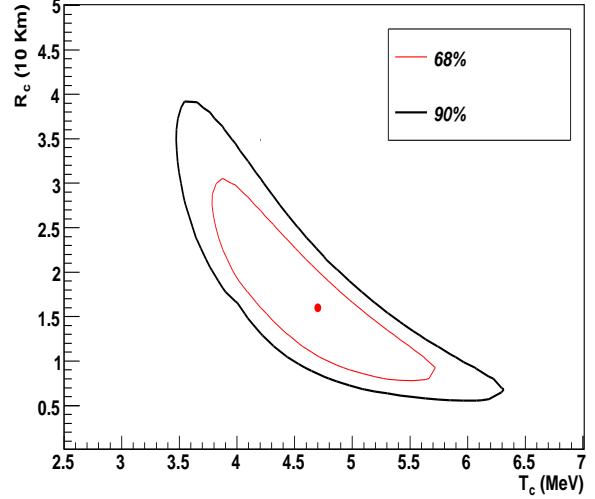


FIG. 3: Two dimensional confidence regions for cooling parameters R_c and T_c of $\bar{\nu}_e$ with the complete emission model (III C).

The 1 sided, 1σ errors for the offset times (obtained by integrating the normalized likelihood profile [80]) are:⁷

$$t_{\text{KII}}^{\text{off}} = 0.{}^{+0.07}_0 \text{ s}, t_{\text{IMB}}^{\text{off}} = 0.{}^{+0.76}_0 \text{ s}, t_{\text{BAK}}^{\text{off}} = 0.{}^{+0.23}_0 \text{ s}. \quad (29)$$

The couples of parameters that are more tightly correlated between them are T_c with R_c , and M_a with T_a . In Fig. 3 and Fig. 4 we report the two dimensional confidence regions for these couples of parameters showing the 90% and 68% contour levels; the correlations are quite evident from the figures. In these figures we focused on the family of solutions with $t^{\text{off}} = 0$ after testing that the other maxima have a very large value of accreting mass, as discussed in Sect. IV B 4.

c. Stability of the best-fit values In order to show the stability of our result we investigated:

- 1) different values for the exponent $m = 1, 3, 4$ (rather than $m = 2$) in Eq. 14, that describes the temporal behavior of positron temperature during accretion;
- 2) the value $k = 10$ (rather than $k = 2$) in Eq. 16 that describes the sharpness of the transition between accretion and cooling phases;
- 3) deviations from the hypothesis of equipartition, by increasing or decreasing the ratio between the $\bar{\nu}_e$ and $\bar{\nu}_x$ luminosities by a factor of 2 [78].

In all cases, the χ^2 changes less than 1 with respect to the best fit result; furthermore, the best fit values of the

⁶ We calculate $\alpha = \prod_{i=1}^{\nu} \int \exp(-x^2/2)/\sqrt{2\pi} dx_i$ for $\sum_{i=1}^{\nu} x_i^2 > \Delta\chi^2$ and taking $\Delta\chi^2$ from Tab. I, where the number of random variables x_i equals the new degrees of freedom $\nu = 3$.

⁷ Only IMB had a reliable measurement of the absolute times; thus, we can use the time of its first event along with $t_{\text{IMB}}^{\text{off}}$ to infer the moment of the beginning of the collapse, presumably coincident with the emission of an intense gravitational wave.

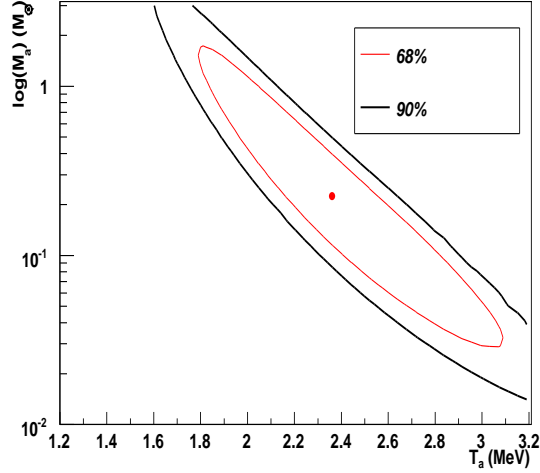


FIG. 4: Two dimensional confidence regions for accretion parameters M_a and T_a of $\bar{\nu}_e$ with the complete emission model (III C).

event	δt_i [s]	E_i [MeV]	LL*	III C
K1	$\equiv 0.0$	20.0	0.69	1.00
K2	0.107	13.5	0.92	1.00
K3	0.303	7.5	0.93	0.81
K4	0.324	9.2	0.95	0.93
K5	0.507	12.8	0.89	0.84
K6	0.686	6.3	0.66	0.10
I1	$\equiv 0.0$	38	0.02	1.00
I2	0.412	37	0.02	0.55
I3	0.650	28	0.05	0.48
B1	$\equiv 0.0$	12.0	0.94	0.99
B2	0.435	17.9	0.70	0.85

TABLE II: Accretion probabilities for the events occurred in the first second; all the other events have a probability to be due to accretion lower than 5%. The first three columns identify the individual events. The last two columns are the probabilities that an event is due to accretion. The model used in the fourth column includes the improvements of Sect. II and following LL sets $M_a = 0.5 M_\odot$; the one used in the fifth column includes also the improvements of Sect. III C.

astrophysical parameters change only within their 1σ errors given in Eq. 28.

d. *On the differences with the parameterization by Lamb and Loredo* To illustrate better the difference between the ECTA model and our final emission model, we show in Tab. II the probabilities of the individual events to be due to accretion. A direct comparison with LL results [36] is not possible, since a similar table is not given there; thus, we repeat their calculation following their prescriptions and make reference to the model LL* described in Sect. IV B 1. The column LL* shows that

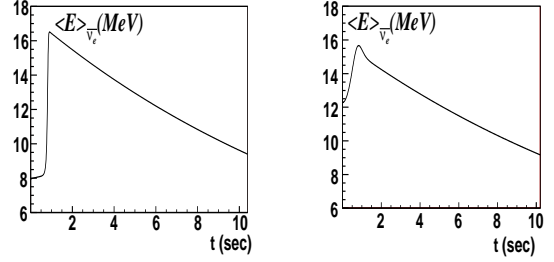


FIG. 5: $\bar{\nu}_e$ mean energy as a function of the time in the LL ECTA model (left panel) and in the III C model (right panel).

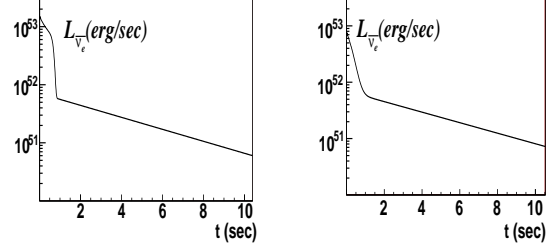


FIG. 6: $\bar{\nu}_e$ luminosity in the LL ECTA model (left panel) and in the III C model (right panel).

the early KII and Baksan events are due to accretion and those by IMB to cooling. This proves that, assuming the Lamb and Loredo ECTA model, the fit takes advantage of the fact that the assumed energy distribution is ‘composite’: the low energy events of KII are explained by the accretion component, the high energy events of IMB instead by the high energy tail due to the cooling component.

The results of our model are shown in the column denoted by III C. Since our model has (by construction) a quasi-thermal spectrum at any time, both KII and IMB early events have a large probability to be due to accretion. The tension between the different energies of KII and IMB events leads to a slightly worse χ^2 (see Tab. I). Finally, we compare in Fig. 5 the mean energy of $\bar{\nu}_e$ in the LL* accretion model, left panel, with the trend of the mean energy in our model III C, right panel, whereas in Fig. 6 we plot the $\bar{\nu}_e$ luminosity obtained with the LL* model (left panel) and the model of Sect. III C (right panel). The features of these curves are similar to those found in typical numerical simulations, see e.g. [13], with the exception of the average energy curve of the LL model that has a very pronounced jump.

V. SUMMARY

We presented an improved analysis of observations of SN1987A by Kamiokande-II, IMB and Baksan. We recall the main points:

1. We collected in Sect. II a large number of technical improvements: new detection cross section, procedure to

include the information on the direction of the events, treatments of the background and of the efficiency. The most relevant improvement is the last one, but none of these changes affect SN1987A data analysis in a crucial manner.

2. We described in Sect. III C the various effects of neutrino oscillations: the oscillations in the star (including the self interaction of neutrinos) and the Earth matter effect. We verified that oscillations with normal hierarchy do not affect the results in an essential manner and discussed the inverted hierarchy case.

3. We proposed in Sect. III a new parameterization of the flux of electron antineutrinos emitted in the accretion phase. We improved on the energy spectrum, and most importantly, on the time-distribution: (a) We prescribed the temperature of the positrons to increase in such a manner that at $t \sim \tau_a$ the average energy antineutrinos is approximatively continuous, that overcomes a shortcoming of the parameterization of [36] noted in [42] and recalled in the Introduction. (b) We also prescribed that the number of neutrons exposed to the positron flux decreases in time more smoothly than as in [36]; in this way the luminosity is also continuous, as expected on general basis. (c) Finally, we avoided the simultaneous presence of cooling and accretion antineutrinos by time-shifting (delaying) the cooling phase of an amount $t \sim \tau_a$, again improving on [36].

4. We demonstrated that the improvements on the parameterization are the most important. The most striking feature is that the best fit parameters are rather similar to the expectations of the Bethe and Wilson scenario. This is in contrast with what happens using the Lamb and Loredò parameterizations of the flux, where it is needed to impose a prior in the analysis to avoid best-fit values outside the physical ranges. Furthermore, our flux leads to smooth luminosity curves and average energies. [The most appealing outcomes of their analysis, such as the neutrino sphere radius resembling the neutron star mass, the duration of the cooling phase ~ 0.5 s, the total amount of emitted energy, are practically unchanged.]

5. We evaluated the errors and the correlations on the parameters and we can rule out the hypothesis of a one-phase model with a significance of 2%.

From these calculations one draws two main messages: an accurate choice of the model for the analysis of SN1987A observations is important; the agreement between the observations and the conventional expectations is more than encouraging in the proposed model. We hope that these results will help to progress further in the understanding of this epochal observation.

Acknowledgments

We thank A. Drago, D.K. Nadyozhin, S. Pastor, and F.L. Villante for useful discussions. The work is partly supported by the MIUR grant for the Projects of National Interest PRIN 2006 “Astroparticle Physics” and

by the European FP6 Network “UniverseNet” MRTN-CT-2006-035863.

APPENDIX: ACCRETION ENERGY SPECTRUM

We derive the equations we used to describe the energy spectrum of accretion $\bar{\nu}_e$.

1. Derivation of Eq. 11

We assume that, during accretion, the antineutrino flux is mostly produced by the weak reaction $e^+n \rightarrow \bar{\nu}_ep$. The rate of this reaction is given by:

$$\Gamma = N_n \int_{m_e}^{\infty} dE_{e^+} \frac{dn_{e^+}}{dE_{e^+}} \beta_e c \int dE_{\nu} \frac{d\sigma_{e^+n}}{dE_{\nu}}, \quad (\text{A.1})$$

where N_n is the number of target neutrons, assumed to be at rest, and where β_e is the positron velocity in natural units. The second integral yields the cross section as a function of the positron energy E_{e^+} . The distribution of the positrons $dn_{e^+} = 2d^3p_e/h^3/(1+\exp[(E_{e^+}-\mu_{e^+})/T_a])$ has a negligible chemical potential [14], thus

$$\frac{dn_{e^+}}{dE_{e^+}}(E_{e^+}) = \frac{8\pi\beta_e}{(hc)^3} g_{e^+}(E_{e^+}, T_a), \quad (\text{A.2})$$

where g_{e^+} is given by Eq. 12. The range of integration of E_{ν} in Eq. A.1 can be easily found from the expression:

$$E_{\nu} = \frac{E_e + \delta_+}{1 + (E_e - p_e \cos \phi)/m_n}, \quad (\text{A.3})$$

where $\cos \phi = \hat{n}_e \cdot \hat{n}_{\nu}$ is the cosine of the angle between the directions of the positron and the antineutrino, $\cos \phi \in [-1, 1]$, and where $\delta_+ = (m_n^2 - m_p^2 + m_e^2)/(2m_n) = 1.293$ MeV $\approx \delta_-$ in Eq. 4. The dependence on the antineutrino energy E_{ν} is as follows:

$$\frac{d\Gamma}{dE_{\nu}} = \frac{8\pi c}{(hc)^3} N_n \int dE_{e^+} \beta_e^2 g_{e^+} \frac{d\sigma_{e^+n}}{dE_{\nu}}. \quad (\text{A.4})$$

The cosine can take all values for fixed $E_{\nu} \geq E_{min}$, with

$$E_{min} = \frac{m_e + \delta_+}{1 + m_e/m_n} \approx 1.803 \text{ MeV}, \quad (\text{A.5})$$

[for smaller E_{ν} , only certain values of $\cos \phi$ around $\cos \phi = -1$ are allowed; but this happens in an interval of E_{ν} wide only about 1 eV]. The range for E_{e^+} is:

$$E_{e^+} = \frac{(E_{\nu} - \delta_+)(1 - \epsilon) - \epsilon \cos \phi \sqrt{(E_{\nu} - \delta_+)^2 - m_e^2(1 + \Delta)}}{1 + \Delta}, \quad (\text{A.6})$$

where $\epsilon = E_{\nu}/m_n$ and $1 + \Delta = (1 - \epsilon)^2 - \epsilon^2 \cos^2 \phi$. From this equation it is clear that the E_{e^+} range is pretty narrow for the energies $E_{\nu} \ll m_n$ in which we are interested; thus, we approximate the expression in Eq. A.4 as:

$$\frac{d\Gamma}{dE_{\nu}} \approx \frac{8\pi c}{(hc)^3} N_n g_{e^+}(\bar{E}_{e^+}(E_{\nu}), T_a) \int dE_{e^+} \beta_e^2 \frac{d\sigma_{e^+n}}{dE_{\nu}} \quad (\text{A.7})$$

where the positron distribution is calculated at the central point of the interval of cosine, namely at $\cos\phi = 0$:

$$\bar{E}_{e^+}(E_\nu) = \frac{E_\nu - \delta_+}{1 - E_\nu/m_n}. \quad (\text{A.8})$$

Eq. A.7 gives the $\bar{\nu}_e$ flux in Eq. 11; the integral will be discussed a while. The advantage of Eq. A.7 is that the dependence on the parameter T_a has been extracted from the integral. The integral can be calculated once forever and we are left with a simpler expression. We checked that, in the most relevant range $T_a = 1 - 4$ MeV, the approximated expression agrees with the correct one at the 1% level for energies $E_\nu < 10 T_a$, and even better when $d\Gamma/dE_\nu$ is integrated in E_ν : indeed, the rate Γ is precise at 0.1%.

2. Derivation of Eq. 13

The cross section in Eq. 13, precisely defined as a numerical approximation of the integral in Eq. A.7, was obtained adapting the calculation of [56] for the inverse beta decay reaction. In fact, the differential cross section

$$\frac{d\sigma_{e^+n}(E_{e^+}, E_\nu)}{dE_\nu} = \frac{G_F^2 \cos^2 \theta_C}{256\pi m_n p_e^2} |\mathcal{M}|^2 (1+r) \quad (\text{A.9})$$

has the *same* matrix element $|\mathcal{M}|^2(s-u, t)$. What changes is the expression of the invariants, now given by: $s-u = 2m_n(E_\nu + E_e) + m_e^2$ and $t = m_p^2 - m_n^2 + 2m_n(E_\nu - E_e)$. The factor $r(E_e)$ describes the small QED radiative corrections; we use expression in [56]. The constant in front to the differential cross section is 2 times smaller than the one for inverse beta decay, because the antineutrino has 1 helicity state whereas the positron has 2. The

characteristic $1/\beta_e$ behavior of an exothermic reaction (such as $e^+n \rightarrow \bar{\nu}_e p$) is compensated by the 2 explicit factors β_e from the positron phase space and from the relative velocity between e^+ and n in the reaction rate, included in σ_{e^+n} .

Our cross section compares well with the approximation of Tubbs and Schramm [81, 82]:

$$\sigma_{e^+n}^{TS} = 1.7 \times 10^{-44} \frac{1 + 3g_A^2}{8} \left(\frac{E_\nu}{m_e} \right)^2, \quad (\text{A.10})$$

with $g_A = -1.27$, since the percentage deviation $100(1 - \sigma_{e^+n}^{TS}/\sigma_{e^+n})$ at $E_\nu = 5, 10, 20, 30$ MeV is just -1%, -2%, -6%, -11% (or -1%, -3%, -7%, -10% when comparing with the approximation of σ_{e^+n} in Eq. 13).

The cross section used in [36] is formally less correct, since it is the same as the above approximation but replacing $g_A^2 \rightarrow |g_A| \approx 1.254$. [This is stated in Eq. (4.5) of LL and can be checked by the value of the energy radiated during accretion, their Eq. (6.2)]. The deviation $100(1 - \sigma_{e^+n}^{LL}/\sigma_{e^+n})$ is not large; for $E_\nu = 5, 10, 20, 30$ MeV is 17%, 16%, 13%, 10% (or 18%, 16%, 13%, 10% when comparing with Eq. 13).

Our parametrization of $\bar{\nu}_e$ spectrum, Eq. 12, differs also for another reason with the one of LL, since we adopt the positron flux calculated in $\bar{E}_e(E_\nu)$ (defined in Eq. A.8), whereas LL use the antineutrino flux calculated in E_ν , namely, $g \rightarrow E_\nu^2/[1 + \exp(E_\nu/T_a)]$. Also this modification acts in the direction of increasing the expected flux. The difference can be quantified by evaluating the integral of the fluxes $\Phi_{\bar{\nu}_e}(T_a) = \int \frac{d\Phi_{\bar{\nu}_e}}{dE_\nu} dE_\nu$: indeed, $1 - \Phi_{\bar{\nu}_e}^{LL}(T_a)/\Phi_{\bar{\nu}_e}(T_a) = 54\%, 35\%, 26\%$ or 19% for $T_a = 1, 2, 3$ or 4 MeV; namely, our flux is significantly larger.

-
- [1] H. T. Janka, A. Marek, B. Mueller and L. Scheck, “Supernova explosions and the birth of neutron stars,” arXiv:0712.3070 [astro-ph].
 - [2] S.E. Woosley and T.A. Weaver, “The evolution and explosion of massive stars. Explosive hydrodynamics and nucleosynthesis”, *Astrophys. J. Suppl.* **101**(1995)181.
 - [3] K. Nomoto *et al.*, “Nucleosynthesis yields of core-collapse supernovae and hypernovae, and galactic chemical evolution”, *Nuclear Physics A*, **777** (2006), 424-458.
 - [4] H. T. Janka, R. Buras and M. Rampp, “The Mechanism of Core-Collapse Supernovae and the Ejection of Heavy Elements,” *Nucl. Phys. A* **718** (2003) 269.
 - [5] A. Burrows, J. Hayes and B. A. Fryxell, “On the nature of core collapse supernova explosions,” *Astrophys. J.* **450** (1995) 830 [arXiv:astro-ph/9506061].
 - [6] C. L. Fryer and K. C. B. New, “Gravitational Waves from Gravitational Collapse,” *Living Rev. Rel.* **6** (2003) 2.
 - [7] K. Kotake, K. Sato and K. Takahashi, “Explosion Mechanism, Neutrino Burst, and Gravitational Wave in Core-Collapse Supernovae,” *Rept. Prog. Phys.* **69** (2006) 971 [arXiv:astro-ph/0509456].
 - [8] S. A. Colgate and R. H. White, “The Hydrodynamic Behavior of Supernovae Explosions,” *Astrophys. J.* **143** (1966) 626.
 - [9] A. Burrows, “Supernova Neutrinos,” *Astrophys. J.* **334** (1988) 891.
 - [10] H. A. Bethe and J. R. Wilson, “Revival of a stalled supernova shock by neutrino heating,” *Astrophys. J.* **295** (1985) 14.
 - [11] D. K. Nadyozhin, “The neutrino radiation for a hot neutron star formation and the envelope outburst problem,” *Astrophys. Space Sci.* **53** (1978) 131.
 - [12] H. T. Janka, A. Marek and F. S. Kitaura, “Neutrino-driven explosions twenty years after SN1987A,” *AIP Conf. Proc.* **937** (2007) 144 [arXiv:0706.3056 [astro-ph]].
 - [13] A. Marek and H. Th. Janka, “Delayed neutrino-driven supernova explosions aided by the standing accretion-shock instability”, preprint astro-ph:0708.3372v1.
 - [14] H.Th. Janka, “Conditions for Shock Revival by Neutrino Heating in Core-Collapse Supernovae,” *A&A*, 368 (2001)

527.

- [15] A. Burrows, D. Klein, R. Gandhi, “The Future of supernova neutrino detection,” *Phys. Rev. D* **45** (1992) 3361.
- [16] R. M. Bionta *et al.* [IMB Collaboration], “Observation of a Neutrino Burst in Coincidence with Supernova SN1987A in the Large Magellanic Cloud,” *Phys. Rev. Lett.* **58** (1987) 1494.
- [17] C. B. Bratton *et al.* [IMB Collaboration], “Angular Distribution Of Events From SN1987A,” *Phys. Rev. D* **37** (1988) 3361.
- [18] K. Hirata *et al.* [Kamiokande-II Collaboration], “Observation of a Neutrino Burst from the Supernova SN1987A,” *Phys. Rev. Lett.* **58** (1987) 1490.
- [19] K. S. Hirata *et al.* [Kamiokande-II Collaboration], “Observation in the Kamiokande-II Detector of the Neutrino Burst from Supernova SN 1987a,” *Phys. Rev. D* **38** (1988) 448.
- [20] E.N. Alekseev, L.N. Alekseeva, I.V. Krivosheina and V.I. Volchenko, “Detection of the neutrino signal from SN1987A in the LMC using the INR Baksan underground scintillation telescope,” *Phys.Lett.B* **205** (1988) 209.
- [21] A. E. Chudakov, Y. S. Elensky and S. P. Mikheev, “Characteristics of the Neutrino Emission from Supernova SN1987A,” *JETP Lett.* **46** (1987) 373 [*Pisma Zh. Eksp. Teor. Fiz.* **46** (1987) 297].
- [22] S. W. Bruenn, “Neutrinos from SN1987A and Current Models of Stellar Core Collapse,” *Phys. Rev. Lett.* **59** (1987) 938; S. H. Kahana, J. Cooperstein and E. Baron, “Neutrinos from Supernova SN1987A,” *Phys. Lett. B* **196** (1987) 259.
- [23] J. N. Bahcall, A. Dar and T. Piran, “Neutrinos from the Supernova in the LMC,” *Nature* **326** (1987) 135; D. N. Spergel, T. Piran, A. Loeb, J. Goodman and J. N. Bahcall, “A Simple Model for Neutrino Cooling of the LMC Supernova,” *Science* **237** (1987) 1471; J. N. Bahcall, T. Piran, W. H. Press and D. N. Spergel, “Neutrino Temperatures and Fluxes from the LMC Supernova,” *Nature* **327** (1987) 682.
- [24] K. Sato and H. Suzuki, “Analysis of Neutrino Burst from the Supernova in LMC,” *Phys. Rev. Lett.* **58**, 2722 (1987); “Total Energy of Neutrino Burst from the Supernova SN1987A and the Mass of Neutron Star Just Born,” *Phys. Lett. B* **196** (1987) 267; “Statistical Analysis of the Neutrino Burst from SN1987A,” *Prog. Theor. Phys.* **79** (1988) 725.
- [25] J. Arafune and M. Fukugita, “Physical Implications of the Kamioka Observation of Neutrinos from Supernova SN1987A,” *Phys. Rev. Lett.* **59** (1987) 367; J. Arafune, M. Fukugita, T. Yanagida and M. Yoshimura, “Neutrino Mass and Mixing Constrained from the LMC Supernova Burst,” *Phys. Lett. B* **194** (1987) 477.
- [26] P.O. Lagage, M. Cribier, J. Rich and D. Vignaud, “MSW Effect and (anti)-Neutrinos from SN1987A,” *Phys.Lett.B* **193** (1987) 127; L. Wolfenstein, “Effects of Matter Oscillations on Supernova Neutrino Flux,” *Phys.Lett.B* **194** (1987) 197; D. Notzold, “MSW Effect Analysis for SN1987A Sets Severe Restrictions on Neutrino Masses and Mixing Angles,” *Phys.Lett.B* **196**, 315 (1987); H. Minakata and H. Nunokawa, “Neutrino Flavor Conversion in Supernova SN1987A,” *Phys.Rev.D* **38** (1988) 3605.
- [27] See J. N. Bahcall, chap. 15 of *Neutrino astrophysics*, Cambridge University Press, 1989 and references therein for a summary of several early analyses.
- [28] V. L. Dadykin, G. T. Zatsepin and O. G. Ryazhskaya, “Events Detected by Underground Detectors on February 23, 1987,” *Sov. Phys. Usp.* **32** (1989) 459.
- [29] H.-T. Janka and W. Hillebrandt, “Neutrino emission from type II supernovae - an analysis of the spectra,” *A&A* **224** (1989) 49.
- [30] J. M. Lattimer, A. Yahil, “Analysis of the neutrino events from supernova 1987A,” *Astrophys. J.* **340** (1989) 426.
- [31] A.Y. Smirnov, D.N. Spergel and J.N. Bahcall, “Is large lepton mixing excluded?,” *Phys. Rev. D* **49** (1994) 1389 [arXiv:hep-ph/9305204].
- [32] P. J. Kernan and L. M. Krauss, “Yet another paper on SN1987A: Large angle oscillations and the electron-neutrino mass,” *Nucl. Phys. B* **437** (1995) 243 [arXiv:astro-ph/9410010].
- [33] B. Jegerlehner, F. Neubig and G. Raffelt, “Neutrino Oscillations and the Supernova 1987A Signal,” *Phys. Rev. D* **54** (1996) 1194 [arXiv:astro-ph/9601111].
- [34] A. Malgin, “Analysis of integral and averaged characteristics of the IMB and Kamioka signals from SN1987A,” *Nuovo Cim. C* **21** (1998) 317.
- [35] C. Lunardini and A. Y. Smirnov, “Neutrinos from SN1987A, Earth matter effects and the LMA solution of the solar neutrino problem,” *Phys. Rev. D* **63** (2001) 073009 [arXiv:hep-ph/0009356].
- [36] T. J. Loredo and D. Q. Lamb, “Bayesian analysis of neutrinos observed from supernova SN 1987A,” *Phys. Rev. D* **65** (2002) 063002.
- [37] M. Kachelriess, A. Strumia, R. Tomas and J. W. F. Valle, “SN1987A and the status of oscillation solutions to the solar neutrino problem,” *Phys. Rev. D* **65** (2002) 073016 [arXiv:hep-ph/0108100].
- [38] H. Minakata and H. Nunokawa, “Inverted hierarchy of neutrino masses disfavored by supernova 1987A,” *Phys. Lett. B* **504** (2001) 301 [arXiv:hep-ph/0010240].
- [39] V. Barger, D. Marfatia and B. P. Wood, “Supernova 1987A did not test the neutrino mass hierarchy,” *Phys. Lett. B* **532** (2002) 19 [arXiv:hep-ph/0202158].
- [40] C. Lunardini and A. Y. Smirnov, “Neutrinos from SN1987A: Flavor conversion and interpretation of results,” *Astropart. Phys.* **21** (2004) 703 [arXiv:hep-ph/0402128].
- [41] M. L. Costantini, A. Ianni and F. Vissani, “SN1987A and the properties of neutrino burst,” *Phys. Rev. D* **70**, 043006 (2004) [arXiv:astro-ph/0403436].
- [42] A. Mirizzi and G. G. Raffelt, “New analysis of the SN 1987A neutrinos with a flexible spectral shape,” *Phys. Rev. D* **72**(2005) 063001.
- [43] C. Lunardini, “The diffuse supernova neutrino flux, star formation rate and SN1987A,” *Astropart. Phys.* **26** (2006) 190 [arXiv:astro-ph/0509233].
- [44] M. L. Costantini, A. Ianni, G. Pagliaroli and F. Vissani, “Is there a problem with low energy SN1987A neutrinos?,” *JCAP* **05** (2007) 014.
- [45] G. Pagliaroli, M. L. Costantini and F. Vissani, “Analysis of Neutrino Signals from SN1987A,” arXiv:0804.4598 [astro-ph], in proceedings of IFAE 2007, ed. by G. Carlini, G. D’Ambrosio, L. Merola, P. Paolucci, G. Ricciardi, page 225.
- [46] Appendix A of F. Vissani and G. Pagliaroli, “How much can we learn from SN1987A events? Or: An analysis with a two-component model for the antineutrino signal,” arXiv:0807.1301 [astro-ph].
- [47] L. Wolfenstein, “Neutrino oscillations in matter,” *Phys. Rev. D* **17** (1978) 2369.

- [48] S. P. Mikheev and A. Y. Smirnov, “Resonance enhancement of oscillations in matter and solar neutrino spectroscopy,” *Sov. J. Nucl. Phys.* **42** (1985) 913 [*Yad. Fiz.* **42** (1985) 1441].
- [49] S. P. Mikheev and A. Y. Smirnov, “Neutrino oscillations in a medium with variable density,” *Sov. Phys. Usp.* **29** (1986) 1155.
- [50] T. K. Kuo and J. T. Pantaleone, “Neutrino Oscillations in Matter,” *Rev. Mod. Phys.* **61** (1989) 937.
- [51] Y. Fukuda *et al.* [Super-Kamiokande Collaboration], “Evidence for oscillation of atmospheric neutrinos,” *Phys. Rev. Lett.* **81** (1998) 1562 [arXiv:hep-ex/9807003].
- [52] Q. R. Ahmad *et al.* [SNO Collaboration], “Direct evidence for neutrino flavor transformation from neutral-current interactions in the Sudbury Neutrino Observatory,” *Phys. Rev. Lett.* **89** (2002) 011301 [arXiv:nucl-ex/0204008].
- [53] K. Eguchi *et al.* [KamLAND Collaboration], “First results from KamLAND: Evidence for reactor anti-neutrino disappearance,” *Phys. Rev. Lett.* **90** (2003) 021802 [arXiv:hep-ex/0411038].
- [54] E. Aliu *et al.* [K2K Collaboration], “Evidence for muon neutrino oscillation in an accelerator-based experiment,” *Phys. Rev. Lett.* **94** (2005) 081802 [arXiv:hep-ex/0411038].
- [55] D. G. Michael *et al.* [MINOS Collaboration], “Observation of muon neutrino disappearance with the MINOS detectors and the NuMI neutrino beam,” *Phys. Rev. Lett.* **97** (2006) 191801 [arXiv:hep-ex/0607088].
- [56] A. Strumia and F. Vissani, “Precise quasielastic neutrino nucleon cross section,” *Phys. Lett. B* **564** (2003) 42.
- [57] A.S. Dighe and A.Yu. Smirnov, “Identifying the neutrino mass spectrum from the neutrino burst from a supernova,” *Phys. Rev. D* **62** (2000) 033007.
- [58] M.L. Costantini, PhD thesis, L’Aquila University, 2007, Sect. 1.2. PDF file available at http://www.infn.it/thesis/thesis_dettaglio.php?tid=1794.
- [59] D. K. Nadyozhin and V. S. Imshennik, “Physics of Supernovae,” *Int. J. Mod. Phys. A* **20** (2005) 6597 [arXiv:astro-ph/0501002].
- [60] D. K. Nadyozhin and I. V. Ostroshchenko, *Astron. Zh.* **57** (1980) 78.
- [61] G.L. Fogli, E. Lisi, D. Montanino and A. Palazzo, “Supernova neutrino oscillations: A simple analytical approach,” *Phys. Rev. D* **65** (2002) 073008.
- [62] J. T. Pantaleone, “Neutrino oscillations at high densities,” *Phys. Lett. B* **287** (1992) 128.
- [63] G. Sigl and G. Raffelt, “General kinetic description of relativistic mixed neutrinos,” *Nucl.Phys.B* **406** (1993) 423.
- [64] J. T. Pantaleone, “Neutrino Flavor Evolution Near A Supernova’s Core,” *Phys. Lett. B* **342** (1995) 250 [arXiv:astro-ph/9405008].
- [65] Y. Z. Qian and G. M. Fuller, “Neutrino-neutrino scattering and matter enhanced neutrino flavor transformation in Supernovae,” *Phys. Rev. D* **51** (1995) 1479 [arXiv:astro-ph/9406073].
- [66] H. Duan, G. M. Fuller, J. Carlson and Y. Z. Qian, “Analysis of Collective Neutrino Flavor Transformation in Supernovae,” astro-ph/0703776.
- [67] V. A. Kostelecky and S. Samuel, *Phys. Lett. B* **318** (1993) 127.
- [68] H. Duan, G. M. Fuller and Y. Z. Qian, “Collective neutrino flavor transformation in supernovae,” *Phys. Rev. D* **74** (2006) 123004 [arXiv:astro-ph/0511275].
- [69] G. G. Raffelt and A. Y. Smirnov, “Self-induced spectral splits in supernova neutrino fluxes,” *Phys. Rev. D* **76** (2007) 081301 [Erratum-ibid. *D* **77** (2008) 029903] [arXiv:0705.1830 [hep-ph]].
- [70] H. Duan, G. M. Fuller, J. Carlson and Y. Q. Zhong, “Neutrino Mass Hierarchy and Stepwise Spectral Swapping of Supernova Neutrino Flavors,” *Phys. Rev. Lett.* **99** (2007) 241802 [arXiv:0707.0290 [astro-ph]].
- [71] G.L. Fogli, E. Lisi, A. Marrone, A. Mirizzi “Collective neutrino flavor transitions in supernovae and the role of trajectory averaging,” *JCAP12* (2007) 010 [arXiv:0707.1998v2 [hep-ph]].
- [72] B. Dasgupta, A. Dighe, A. Mirizzi “Identifying neutrino mass hierarchy at extremely small θ_{13} through Earth matter effects in a supernova signal,” [arXiv:0802.1481v2 [hep-ph]].
- [73] A. Esteban-Pretel, S. Pastor, R. Tomas, G.G. Raffelt, G. Sigl “Mu-tau neutrino refraction and collective three-flavor transformations in supernovae,” *Phys. Rev. D* **77** (2008) 065024 [arXiv:0712.1137 [astro-ph]].
- [74] A. Esteban-Pretel, A. Mirizzi, S. Pastor, R. Tomas, G.G. Raffelt, P.D. Serpico, G. Sigl “Role of dense matter in collective supernova neutrino transformations,” [arXiv:0807.0659v1 [astro-ph]].
- [75] A. Strumia and F. Vissani, “Neutrino masses and mixings and...,” arXiv:hep-ph/0606054., a review regularly updated on the web.
- [76] F. Cavanna, M.L. Costantini, O. Palamara, F. Vissani, “Neutrinos as astrophysical probes,” *Surveys HEP* **19** (2004) 35.
- [77] As in Fig.A1 of N.Y. Agafonova *et al.*, “Study of the effect of neutrino oscillations on the supernova neutrino signal in the LVD detector,” *Astropart. Phys.* **27** (2007) 254.
- [78] M.T. Keil, G.G. Raffelt and H.T. Janka, “Monte Carlo study of supernova neutrino spectra formation,” *Astrophys. J.* **590** (2003) 971.
- [79] G. Pagliaroli, M. L. Costantini, A. Ianni and F. Vissani, “The first second of SN1987A neutrino emission,” arXiv:0705.4032 [astro-ph].
- [80] G. Cowan, “Statistical Data Analysis”, Oxford Science Publications 1998.
- [81] D. L. Tubbs and D. N. Schramm, “Neutrino Opacities At High Temperatures And Densities,” *Astrophys. J.* **201** (1975) 467.
- [82] H.-T. Janka, R. Moenchmeyer, “Anisotropic neutrino emission from rotating protoneutron stars,” *A&A* **209** (1989) L5.